ANALYSIS OF THE INFLUENCE OF THE SPEED OF IMPACT AGAINST AN OBSTACLE ON THE DYNAMIC LOADS ACTING ON OCCUPANTS OF AN AUTOMOTIVE VEHICLE WITH BODY-ON-FRAME DESIGN OF THE LOAD-BEARING STRUCTURE

LEON PROCHOWSKI[1], ANDRZEJ ŻUCHOWSKI[2], KAROL ZIELONKA[3]

Military University of Technology, Automotive Industry Institute

Summary

The dynamic loads acting on a human body during a road accident may cause bodily injuries. The values of such loads measured on test dummies make it possible to predict the effects of the loads on vehicle occupants, with the prediction being based on biomechanical modelling. The dynamic loads were analysed with making use of experimental results of tests where an automotive vehicle came into a head-on collision with an obstacle. In the test vehicle, a Hybrid III test dummy provided with a set of sensors was held with seat belts in the driver's position. By using the experimental results and the determined extreme values of dynamic loads, the dependence of the dynamic loads on the speed of vehicle impact against an obstacle is searched. The knowledge of this dependence will facilitate the prediction of values of dynamic loads and the resulting dangers to the human body that would arise from road accidents.

The tests were carried out on an off-road passenger car, where a frame makes a basis of the entire load-bearing structure, i.e. connects all the vehicle components and systems into a self-contained whole and supports the vehicle body. Vehicles with load-bearing structures of this type predominate among those used for military applications. Results of crash tests of such vehicles are rarely published.

Keywords: transport safety, crash tests, off-road passenger cars, dynamic loads of vehicle occupants.

[1] Military University of Technology, Departament of Mechanical Engineering, Vehicles Institute, 2 Gen. S. Kaliskiego Street, 00-908 Warszawa, e-mail: lprochowski@wat.edu.pl, ph.: +48 22 683 78 66

[1] Military University of Technology, Departament of Mechanical Engineering, Vehicles Institute, 2 Gen. S. Kaliskiego Street, 00-908 Warszawa, e-mail: azuchowski@wat.edu.pl, ph.: +48 22 683 74 54

[3] Karol Zielonka, Automotive Industry Engineering, Vehicle Safety Laboratory, 55 Jagiellońska Street, 03 – 301 Warszawa, e-mail: k.zielonka@pimot.org.pl, ph.: +48 22 777 71 41

1. Introduction

When a vehicle hits a rigid obstacle, a vehicle deformation process takes place. The course and size of the deformation chiefly depends on the impact speed and the rigidity of the vehicle load-bearing structure [1]. The process of deformation of the load-bearing structure is the main factor of dissipation of the impact energy; therefore, it has decisive influence on the transmission of dynamic loads from the zone of contact between the vehicle and the obstacle, through vehicle structure components, to the occupants.

In passenger cars, monocoque bodies predominate. Conversely, off-road passenger cars usually have body-on-frame design. In the latter case, the frame provides a basis for the load-bearing system and it makes the vehicle structure far more rigid. In most cases, ladder frames are used, where the longitudinal members are parallel or almost parallel to the longitudinal symmetry plane of the vehicle. Sometimes, semi-monocoque bodies are used, where the load-bearing frame is welded to the body floor (ladder-boxed chassis, e.g. Jeep Cherokee).

This study was undertaken to define and analyse the dependence between the speed of vehicle impact against an obstacle and the dynamic loads arising in vehicles with body-on-frame design of the load-bearing structure. The knowledge of this dependence will make it easier to predict the dangers to which vehicle occupants might be exposed during a road accident. The analysis of dynamic loads acting on the human body as described in a subsequent part of this paper was carried out with taking as a basis results of experimental tests of a ladder-framed off-road passenger car.

Vehicles with load-bearing structures of this type predominate among those used for military applications. Results of crash tests of such vehicles are rarely published, while being of great significance for positioning the crew and for improving the passive safety systems of vehicles of this category. This is the more so important that the collisions taking place during straight-on drive make 67% of accidents of vehicles like these [2].

2. Object of testing and the measuring system

The vehicle subjected to tests was an off-road passenger car Tarpan-Honker having a ladder frame. The car body was a one-piece welded structure fixed on the frame with 9 fastener units. The occupants of front seats were offered three-point seat belts. The seat belt anchorage points were arranged in the vehicle body and they were not connected with the seats. During the measurements, a Hybrid III test dummy was placed on a driver's seat and held in position with seat belts tightened with a force of 50 N.

The experiment, during which the vehicle frontally hit a non-deformable obstacle, i.e. a concrete barrier, was prepared and carried out at the Automotive Industry Institute in Warsaw. It included measurements of the following quantities:

- Acceleration (deceleration) of the head and torso;
- Forces arising in the neck and thighs of the dummy;
- Forces arising in the seat belts.

Fig. 2.1. Position of the test dummy with sensors in the car.

The position of the dummy in the car is shown in Fig. 2.1. The sensors were so positioned in the dummy and car that the direction of the main measuring axis of each sensor was identical with that of the car motion before the collision with the obstacle.

The measuring system used met requirements of the relevant standard [3]. The measurements were carried out with a signal sampling frequency of 10 kHz.

To pursue the objective of the study, three experiments were carried out, during which the same vehicle hit the concrete barrier with speeds of 4, 10, and 43 km/h in succession. After the impacts with speeds of 4 and 10 km/h, only minor deformations of the front bumper beam could be seen; the impact with a speed of 43 km/h caused destructive deformations of the vehicle frame and body. In consequence, no further tests could be carried out on this car.

3. Filtering of the measurement signals

The measurement results at crash tests may be treated as a realisation of a random function X(t), where the independent variable is time t. Every value of this realisation, at an

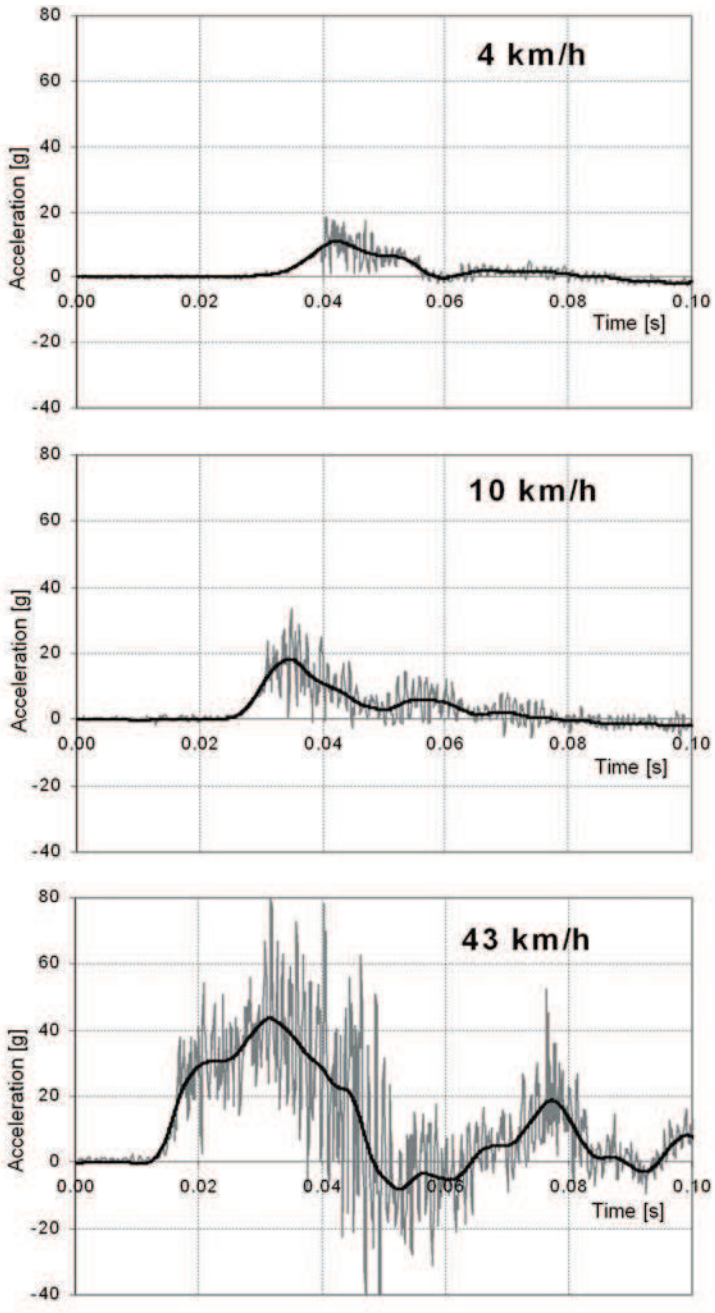

Fig. 3.1. Example of the time histories of measurement signals before and after filtering (100 Hz); longitudinal acceleration of the vehicle body (in the Ox direction).

arbitrary value of t, is a random variable. To examine the properties of a random function, including the extreme values of the function, we should carry out n separate experiments (measurements), in result of which we would obtain a set of realisations x(t) of the random function X(t). For crash tests, this is actually impossible because of their destructive nature. A characteristic feature of the tests carried out is the finite short duration time of the realisation. However, the realisation x(t) obtained in result of an experiment defines, with a degree of approximation, the properties of the random function and characterises the process under examination.

Fig. 3.1 shows examples of realisations of the measured time histories of acceleration (fine line).

The time histories, showing high dynamics and depending on a huge number of factors that are determined by vehicle features and by the course of the experiment, contain not only the usable signal being the matter of interest but also a number of interfering signals of individual nature depending on a specific experiment. Thus, the realisation determined is a sum of the usable signal and the interference (noise):

$$x(t) = x_u(t) + \beta(t) \tag{1}$$

A part of the interference may be removed by filtering. At the filtering thus understood, it is important that the spectral density of the signal and the noise should not overlap. This may be easily assessed on the grounds of results of a spectral analysis. The frequency structure of the signal examples is shown in Fig. 3.2, where estimators of the spectral

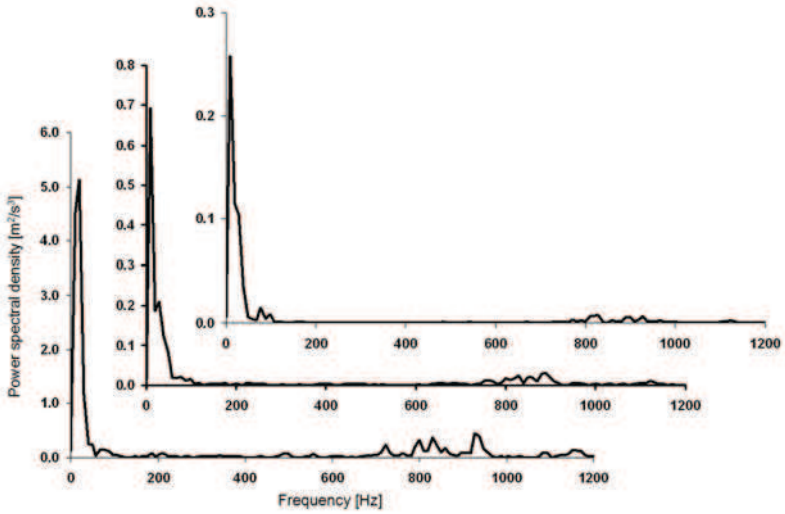

Fig. 3.2. Estimator of the power spectral density of three acceleration vs. time curves (the signals as shown in Fig. 3.1), with the curves for impact speeds of 4, 10, and 43 km/h arranged in the order from top to bottom.

density of the acceleration signal measured on the vehicle floor during the impact against the obstacle, calculated with the use of the FFT method, have been plotted.

The predominating frequency constituents can be seen in the 10 ÷ 20 Hz frequency band. The figure shows the reasonability of low-pass filtering with a cut-off frequency of 100 Hz.

The results of filtering the signals, obtained with the use of CFC 60 filters, are represented in Fig. 3.1. by heavy lines. The filters used were in conformity with the crash test methods recommended in the relevant standard [3]. For the CFC 60 filter, the cut-off frequency was 100 Hz.

In this case, the filtering problem is similar to the problem of estimation of the average value on a given time interval. For the integral average on the interval (T, T)

$$m_x(t) = \frac{1}{2T}\int_{-T}^{T} x(t+\tau)d\tau \tag{2}$$

the parameter is the length of the so-called "sliding interval" in the operation of integration (2T) [4, 5, 6].

The filtering procedure as described above was applied to all the time histories cited in this paper. The extreme values, determined from the time histories obtained by filtering the values measured during crash tests, are commonly used to assess the properties of the vehicles examined. This is a normal practice, although the extreme values have the nature of a random variable. For this reason, it is difficult to achieve adequate repeatability in experiments carried out on successive specimens of vehicles of the same type. However, the scatter of these values is usually small thanks to the operation of determination of average values over the whole length of the integration interval (2) [1].

4. Dynamic loads acting on the vehicle driver. Measurement results and an analysis

The filtered time histories were analysed in a systematised order. This order should help in revealing the actual matter of interest, i.e. the influence of vehicle speed on the time history and values of the dynamic loads acting on vehicle occupants.

The film records of dummy's movements show that the seat belt effectively held the dummy on the seat and that dummy's head did not come into contact with vehicle components at small speeds of vehicle impact against the barrier (4 and 10 km/h) (see Fig. 4.1). At the impact speed of 43 km/h, the dummy moved in relation to the seat and hit its head on vehicle parts (see Fig. 4.2).

Fig. 4.1. Test dummy in the car during the impact against the obstacle; the maximum displacement of the dummy at the impact speed of 4, 10, and 43 km/h, respectively, has been shown.

4.1. Results of measurements of the dynamic loads acting on the head

A set of three acceleration sensors was installed in the centre of mass of dummy's head. The directions of the sensor measurement axes are shown in Fig. 4.2. The acceleration time histories (representing three principal components and the resultant) are presented in Fig. 4.3. Proceeding from top to bottom, the four separate graphs included in Fig. 4.3 represent the following:

- Longitudinal component a_{Gx}, measured in the direction of car motion;
- Transverse component a_{Gy}, perpendicular to the direction of car motion;
- Vertical component a_{Gz};
- Resultant acceleration a_G.

The word "direction" used here refers to the original position of the sensors and the dummy. Each of the four graphs in Fig. 4.3 includes three curves, which represent results of the measurements carried out at the car impact speeds of 4, 10, and 43 km/h.

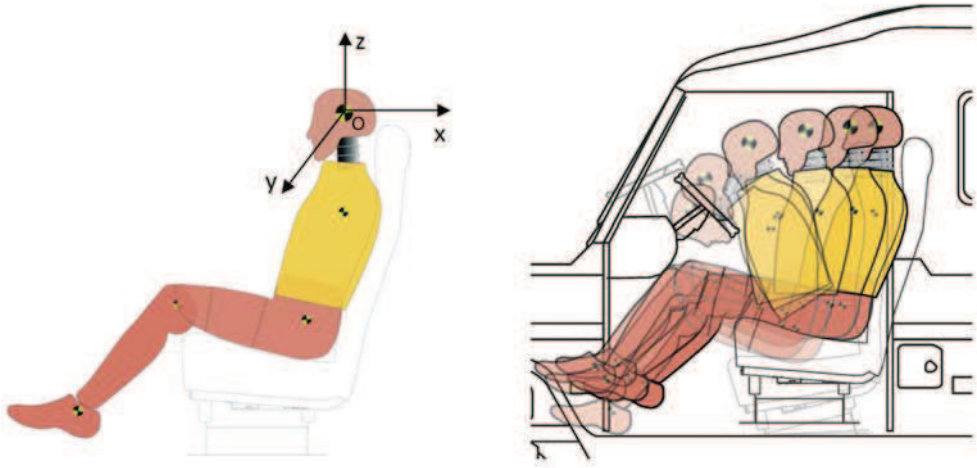

Fig. 4.2. Directions of measurement axes of the sensors installed in dummy's head and successive phases of dummy's movement (recorded at 20 ms time intervals) at the impact speed of 43 km/h [7].

The predominating acceleration values were measured with the use of the sensor of the component a_{Gx}; at the initial measurement stage, this acceleration was identical with the longitudinal acceleration (i.e. its direction was identical with the direction of vehicle motion). During the measurement, however, dummy's head was tilting forward (see Fig. 4.2) and the sensor was changing its position accordingly in relation to the direction of vehicle motion. In the time history a_{Gx} (t), we can see that the highest deceleration values occurred when the head hit parts of vehicle interior equipment (t = 0.10 ÷ 0.12 s); afterwards, the acceleration increased again at t = 0.22 ÷ 0.24 s, i.e. when the head struck the headrest during the return motion.

The noticeable growth in the extreme values of the longitudinal component of the head acceleration a_{Gx} was almost proportional to the growth in the vehicle impact speed:

- at v = 4 km/h, the extreme value of acceleration a_{Gx} was 4 g;
- at v = 10 km/h, 9 g;
- at v = 43 km/h, 40 g.

The maximum values of the time histories of the resultant acceleration shown in the fourth part of Fig. 4.3 and defined by the formula

$$a_G(t) = \sqrt{a_{Gx}^2(t) + a_{Gy}^2(t) + a_{Gz}^2(t)} \tag{3}$$

were as follows:

- at v = 4 km/h, the maximum value of acceleration a_G was 4 g;
- at v = 10 km/h, 9 g;
- at v = 43 km/h, 50 g.

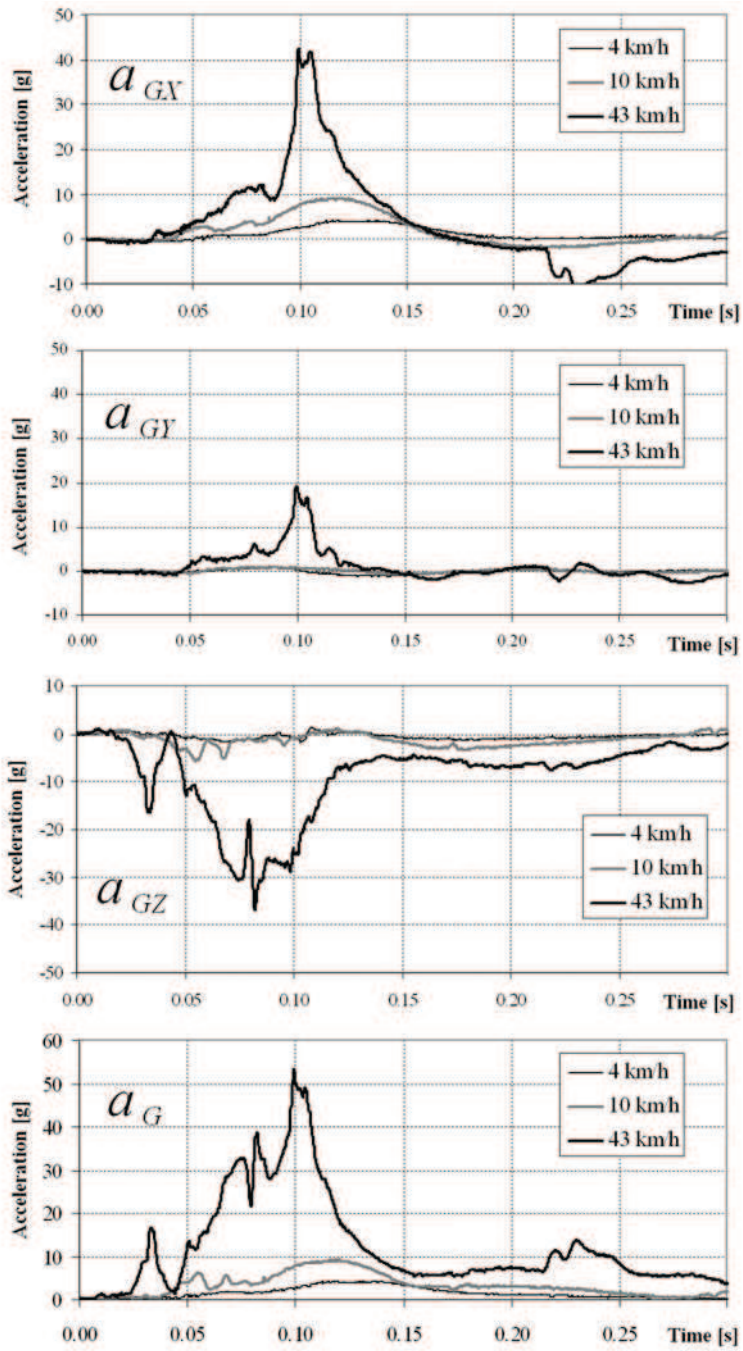

Fig. 4.3. Dummy's head acceleration vs. time curves, representing (from top to bottom) the acceleration components a_{Gx}, a_{Gy}, and a_{Gz}, and the resultant acceleration a_G, respectively.

The sense of extreme values given above is to provide information about the nature of changes in the time histories under consideration depending on the vehicle impact speed, in accordance with the physical sense of the filtering operation and of its smoothing properties.

4.2. Results of measurements of the dynamic loads acting on the torso

The movement of dummy's torso was caused by the effect of increasing values of deceleration $a_T(t)$ and the resulting inertia forces, which are balanced in a significant part by seat belt reactions. Time histories of the following acceleration values, measured at the centre of mass of dummy's torso, are presented in Fig. 4.4, proceeding from top to bottom:

- Component $a_{Tx}(t)$, measured in the direction of car motion (longitudinally);
- Realisations of the resultant acceleration $a_T(t)$, calculated similarly as it was in the case of that defined by (3).

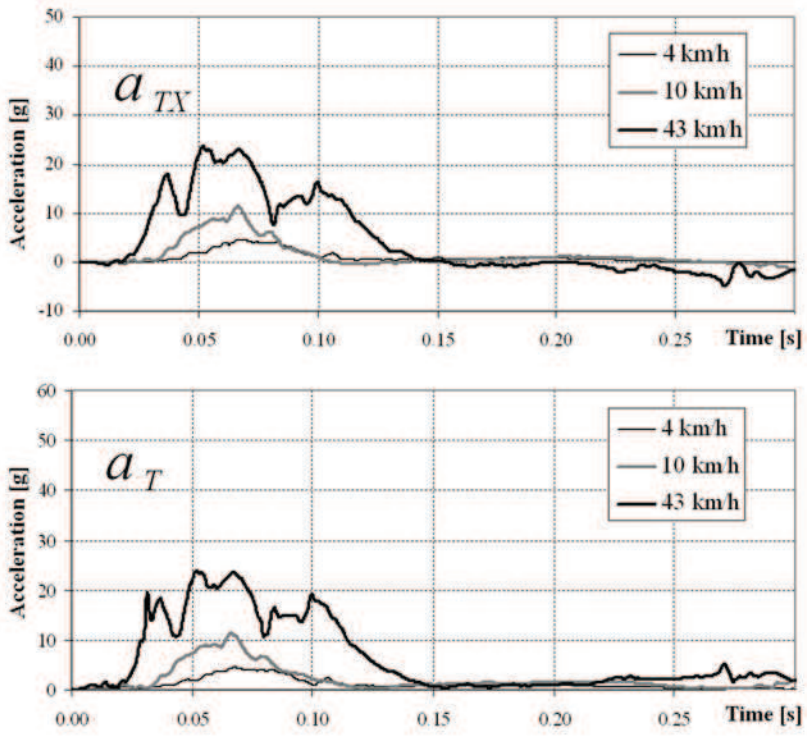

Fig. 4.4. Dummy's torso acceleration vs. time curves, representing (from top to bottom) the acceleration values a_{Tx} and a_T, respectively.

The torso movement caused by inertia forces was favourably restrained by seat belts; therefore, the angular and transverse displacements of the torso were small. For this reason, the acceleration components a_{Ty} (t), and a_{Tz} (t) measured in the transverse and vertical directions, respectively, were small and, in consequence, they have been ignored in Fig. 4.4. The rate of growth of the longitudinal torso accelerations was lower (depending on the impact speed) than that observed on dummy's head and the vehicle frame [7]. With increasing impact speeds, the extreme acceleration values grew as specified below:

- at v = 4 km/h, the extreme value of acceleration a_{Tx} was 4 g;
- at v = 10 km/h, 10.5 g;
- at v = 43 km/h, 23.5 g.

The maximum values of the resultant torso acceleration, determined from the time histories filtered according to formula (2), grew with the increasing impact speeds as shown below:

- at v = 4 km/h, the maximum value of acceleration a_G was 4.2 g;
- at v = 10 km/h, 11 g;
- at v = 43 km/h, 24.5 g.

The dummy's torso movement that took place during the head-on impact of the car against the obstacle initially consisted in deviation from the backrest (with growing tilt angle, Fig. 4.2) and resulted in increasing tension in the chest/shoulder portion of the seat belt. Increasing values of deceleration a_T (t) and the resulting inertia forces exerted by dummy's torso on the seat belt stretched the belt and caused the dummy to be moved back at the final stage of the vehicle impact against the obstacle.

The tension forces in the seat belt were measured with the use of load cells P1, P2, and P3, situated as shown in Fig. 4.5.

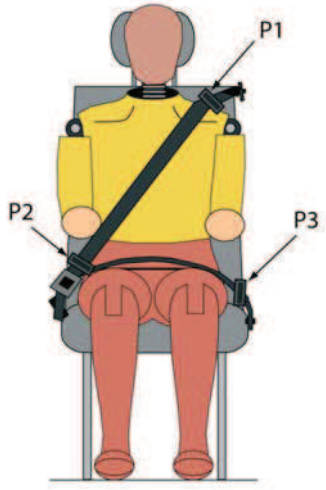

Fig. 4.5. Locations of load cells P1, P2, and P3 in the seat belt.

The time histories of the forces in the three-point seat belt as presented in Fig. 4.6 resulted from the influence of dummy's torso on the belt. After the head hit the dashboard, the tension in the chest/shoulder portion of the seat belt (load cells P1 and P2) almost did not grow any longer because the inertia force acting on the torso was partly balanced by the reaction force exerted by the dashboard on dummy's head deeply tilted down. In this situation, the time histories of the forces in the chest/shoulder portion of the seat belt recorded at the impact speeds of 4 and 10 km/h are definitely different from those recorded at the speed of 43 km/h, where the process of growth of forces P1 and P2 was noticeably hampered in the time period of t = 0.05÷0.10 s. At the impact speed of 43 km/h, the force vs. time curves as presented in Fig. 4.6 were significantly affected by the functioning of seat belts and deformation of the car body in the area of seat belt anchorage points.

Differences in the time histories and extreme values of forces P1 and P2 in the chest/shoulder portion of the seat belt can be explained by the effect of friction forces between the belt and the dummy's clothes. The tension forces in the lap portion of the belt resulted from the influence of the inertia forces acting on the dummy and the reactions applied to dummy's legs resting on the vehicle floor. Hence, these forces strongly (almost proportionally) increased with the speed of vehicle impact against the obstacle:

- at v = 4 km/h, the maximum force in the lap belt portion was 50 daN;
- at v = 10 km/h, 140 daN;
- at v = 43 km/h, 580 daN.

4.3. Results of measurements of the dynamic loads acting on the neck

The directions of measurement axes of the load cells placed in dummy's neck are shown in Fig. 4.7. The decisive role in the causing of injuries to the cervical section of the vertebral column is played by the shearing forces (i.e. the forces perpendicular to the z axis) F_x and F_y. Injuries may also result from excessive compression of the cervical vertebrae, caused by force F_z.

Fig. 4.8 consists of three separate graphs that define the force acting in dummy's neck. The graphs represent the following:

- Longitudinal component F_x, measured in the direction of car motion;
- Vertical component F_z;
- Resultant shearing force F_W, which is important for the injury generation process and is defined by a formula

$$F_W = \sqrt{F_x^2 + F_y^2} \tag{4}$$

The measured values of the component force F_y (t) were so small that they have been ignored in Fig. 4.8.

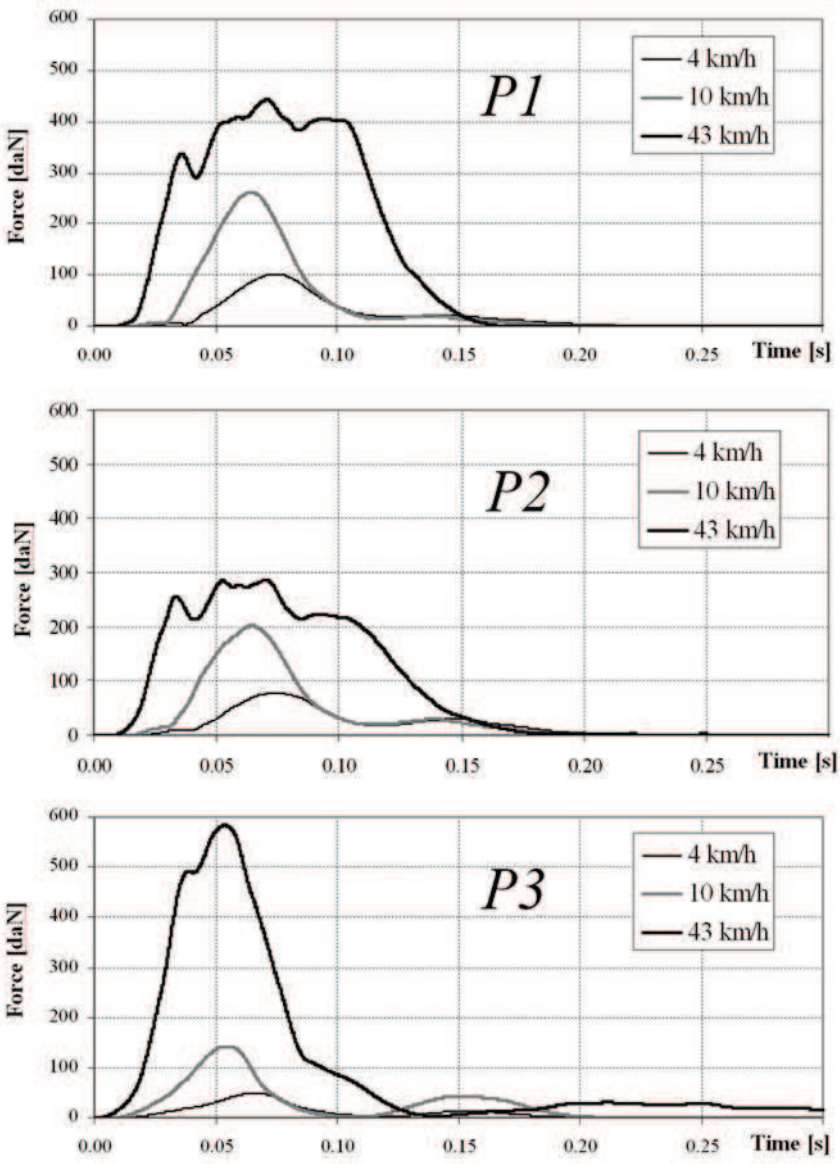

Fig. 4.6. Time histories of the forces stretching the seat belt webbing in the chest/shoulder portion (P1, P2) and the lap portion (P3) of the belt.

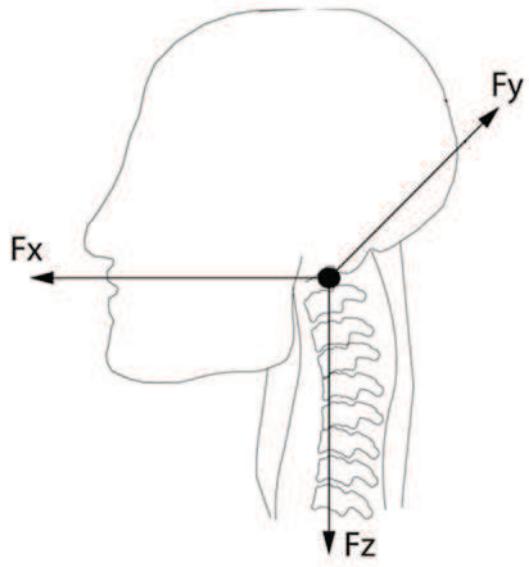

Fig. 4.7. Directions of measurement axes of the load cells installed in dummy's neck.

The forces that constitute the load of dummy's neck strongly depend on the time history of deceleration $a_G(t)$ and on changes in the positions of dummy's head and torso in relation to each other. The rate of growth of the extreme longitudinal forces arising in dummy's neck was visibly lower than that of the impact speeds applied at successive car tests, as it can be seen in the comparison given below:

- at v = 4 km/h, the extreme value of force $F_x(t)$ in the neck was 12 daN;
- at v = 10 km/h, 26 daN;
- at v = 43 km/h, 80 daN.

The maximum values of the resultant shearing force also increase with growing vehicle impact speed:

- at v = 4 km/h, the extreme value of resultant force $F_W(t)$ was 13 daN;
- at v = 10 km/h, 26 daN;
- at v = 43 km/h, 85 daN.

The steep growth in the dummy's head tilt angle and the contact of the head with the dashboard during the vehicle impact against the obstacle at the speed of 43 km/h resulted in an increase in the compressive component force (axial force $F_z(t)$) in the neck, visible in Fig. 4.8. The maximum values of the compressive force in the neck were as specified below:

- at v = 4 km/h, the maximum value of force $F_z(t)$ in the neck was 10 daN;
- at v = 10 km/h, 21 daN;
- at v = 43 km/h, 135 daN.

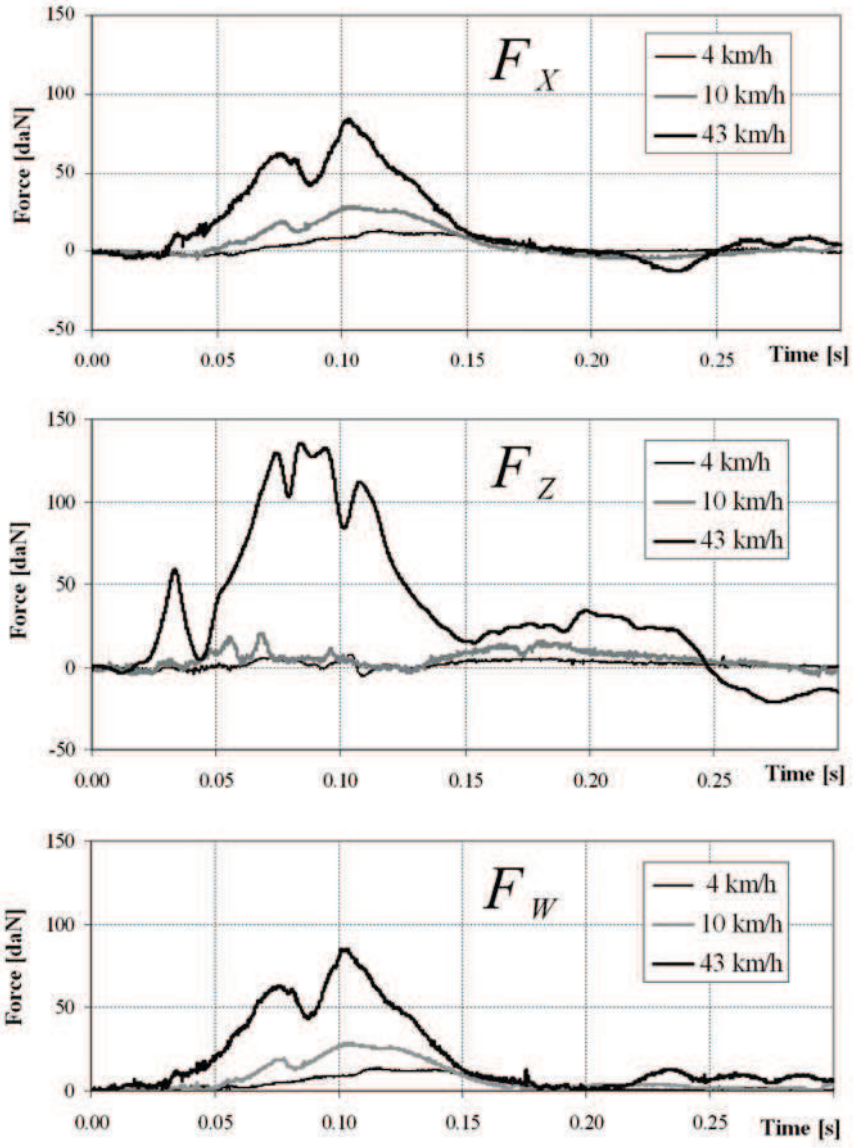

Fig. 4.8. Time histories of the measured forces acting in dummy's neck.

4.4. Results of measurements of the dynamic loads acting on the legs

The sensors (load cells) installed in dummy's legs made it possible to measure the time histories of the loads acting on thighs of the dummy placed on the vehicle seat and held in position with a seat belt.

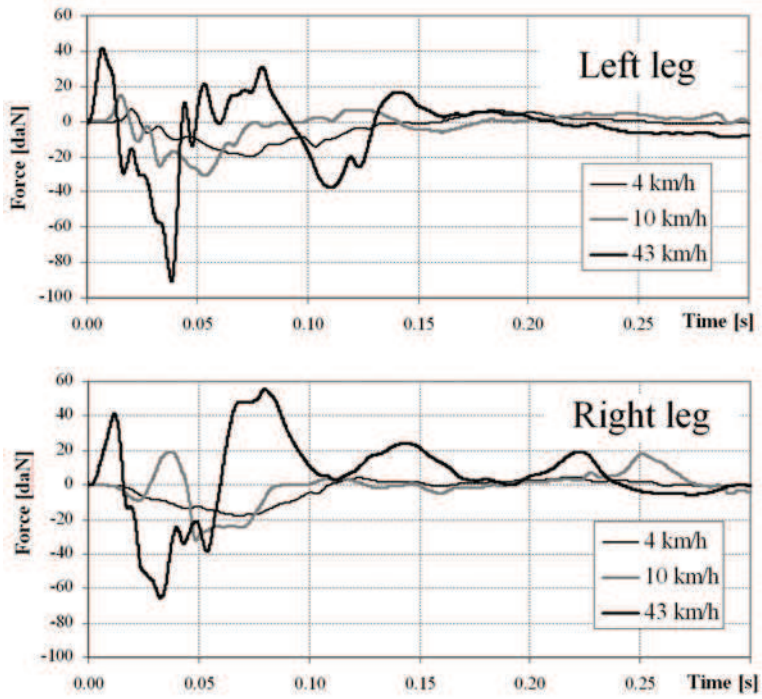

Fig. 4.9. Time histories of the forces acting on dummy's left and right leg.

The observed time histories of the dynamic loads of dummy's legs (Fig. 4.9) show significant variability, which results from the effect of dummy's torso inertia forces and the influence of the process of deformation of vehicle body floor on dummy's feet. Of course, the seat belt restraints the dummy's hip movement in relation to the seat and this may favourably reduce the dynamic loads of thigh bones. The observed extreme values of the forces in the thighs increase at a rate lower than that of the values of the vehicle impact speed. The example spans of the values of these forces are presented below:

- at v = 4 km/h, the span of extreme forces in the left thigh was 28 daN;
- at v = 10 km/h, 45 daN;
- at v = 43 km/h, 135 daN;

and

- at v = 4 km/h, the span of extreme forces in the right thigh was 18 daN;
- at v = 10 km/h, 52 daN;
- at v = 43 km/h, 120 daN.

5. Analysis of the influence of vehicle impact speed on the dynamic loads acting on the driver

The loads acting on a human body may cause bodily injuries. The loads measured on test dummies make it possible to predict the effects of the loads on vehicle occupants, with the prediction being based on biomechanical modelling. The measurement results described previously were used for attempting to prepare a synthetic evaluation of the loads based on their extreme values, by searching for the dependence of the loads on the speed of vehicle impact against an obstacle. The conclusions drawn from the curve representing the said dependence provide important information for vehicle designers and users regarding safe location of the crew, introduction of appropriate personal protection means for vehicle occupants, and effectiveness of the equipment used hitherto for this purpose.

Due to short duration and variability of the processes that take place when a vehicle hits an obstacle, the factors that directly cause an injury, such as the actual stress level, are not analysed; instead, physical quantities related to the body movement, such as displacement, velocity, or acceleration (measured with the use of test dummies), are successfully used at the research work carried out in this field. Criteria based on results of measurements of the forces and moments causing deformations of the human body are employed as well [8].

In consideration of the above, the values obtained from measurements were subjected to a standardisation procedure, with the values of the coefficient of growth of the load being calculated on these grounds

$$y_i(v_k) = \frac{4}{d_i(v_1)} d_i(v_k) \tag{5}$$

where:

v_k represents successive values of the impact speed, i.e.

v_1 = 4 km/h, v_2 = 10 km/h, and v_3 = 43 km/h;

$d_i(v_k)$ represents the extreme values obtained from the d_i measurement of the specific physical quantity at the impact speed v_k.

The number "4" in the numerator of formula (5) is equal to the numerical value of the reference speed v_1 and, simultaneously, has the meaning of a scale factor for the graphs plotted.

The values of the coefficient of growth of the dummy load, calculated for the accelerations of dummy's head and torso and for the forces in dummy's neck and thighs, are presented in Figs. 5.1 ÷ 5.3; then, these values were subjected to approximation by a polynomial in the form of

$$y = b_2 v^2 + b_1 v + b_0 \tag{6}$$

where:

y is the coefficient of growth of the load and

v is the speed of vehicle impact against the obstacle in km/h.

The curves representing the approximation function obtained have been plotted with a full line. The values of the coefficient of growth of the load, determined for the frame as the predominating component of the load-bearing structure of the vehicle under tests with the use of the results obtained from the experiment analysed, have also been shown in the graphs. These calculation results were also approximated by function (6) and the curve thus obtained was plotted with a dashed line. The curves plotted in Fig. 5.1 are based on 33 points calculated with the use of equation (5) and the values previously given in this paper. They show the general relationships between the growth of dynamic loads of the dummy (head, neck, torso, thighs) and the load measured on the frame of the off-road passenger car during the car impact against the obstacle.

Some more detailed conclusions may be drawn from an analysis of the approximation function curves plotted in Figs. 5.2 and 5.3. It can be seen from Fig. 5.2 that the rate of growth of dynamic loads of the head exceeds that of the frame; for the neck, the dynamic loads grow at a rate lower than that determined for the load-bearing system of the car.

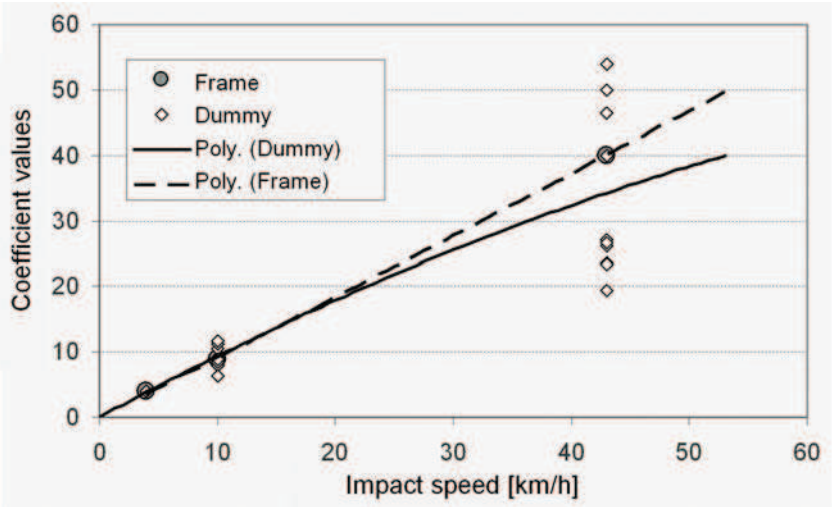

Fig. 5.1. Values of the coefficient of growth of the dynamic load measured in the dummy and on the vehicle frame and polynomial approximations of these values.

It should be noticed that the predominating extreme values of the loads occurred in both cases at the instants when the head hit parts of the vehicle interior.

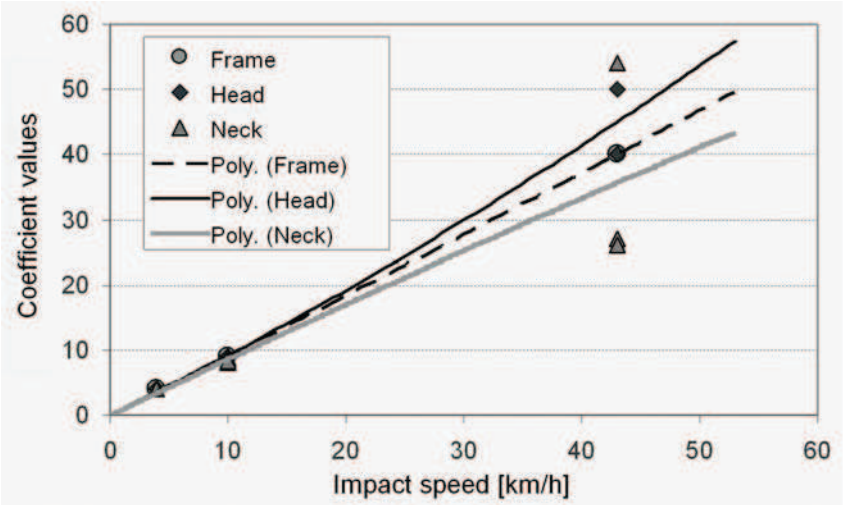

Fig. 5.2. Values of the coefficient of growth of the dynamic loads measured in dummy's head and neck and on the vehicle frame (18 points in total) and polynomial approximations of these values.

The approximation function curves plotted in Fig. 5.3 (approximation with a polynomial of degree 2 and with a power function) show that the rates of growth of dynamic loads of dummy's torso and thighs are visibly lower than that observed on the frame.

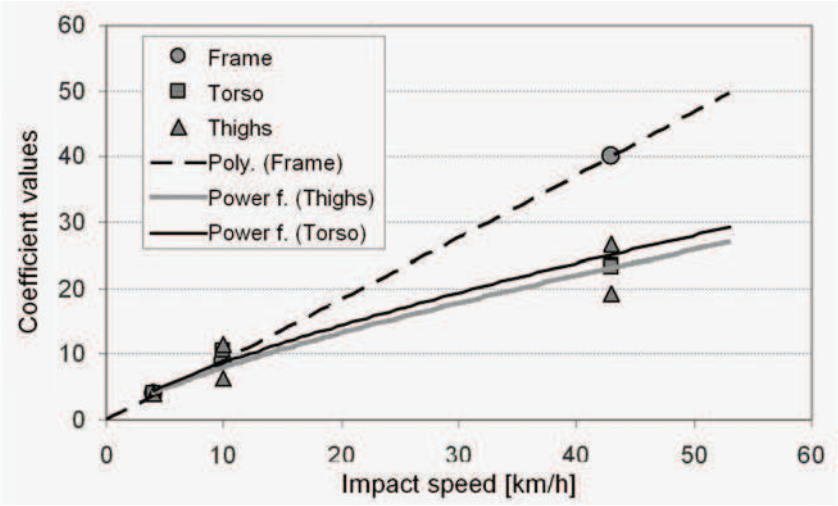

Fig. 5.3. Values of the coefficient of growth of the dynamic loads measured in dummy's torso and thighs and on the vehicle frame and polynomial approximations of these values.

Calculations carried out have showed that high values of the coefficient of convergence of the approximation have been obtained for the approximation functions going through the origin of coordinates (0, 0) (cf. Table 5.1).

Table 5.1. Equations of the functions that approximate the dependences of the coefficient of growth of the loads measured in the dummy and on the frame on the impact speed, shown in Figs. 5.1 ÷ 5.3, and values of the coefficient of convergence

Location of the measurement point	Approximation function	R^2
Frame	$y = 0.0007v^2 + 0.901v$	0.999
Dummy	$y = -0.0043v^2 + 0.979v$	0.791
Dummy's head	$y = 0.0038v^2 + 0.881v$	0.975
Dummy's neck	$y = -0.001v^2 + 0.871v$	0.778
Dummy's torso	$y = 1.639v^{0.726}$	0.966
Dummy's thighs	$y = 1.523v^{0.725}$	0.926

The curves representing the functions approximating the dependence of the dynamic loads acting on vehicle occupants on the impact speed indicate that the factors of decisive importance are the process of deformation of the vehicle load-bearing structure and the characteristics of the vehicle components through which loads are transmitted from the zone of contact between the vehicle and the obstacle to the human body. In vehicles of construction such as considered in this paper, the loads transmitted to occupant's body actually come from the loads of vehicle frame. For the head as a solid of significant freedom of movement in relation to the torso and vehicle body, the rate of growth of dynamic loads exceeded that recorded for the frame. For the other dummy's parts, to which dynamic loads were transmitted though body-to-frame fastener units, vehicle body, and seats, the rate of growth of such loads with increasing impact speeds was lower than that recorded for the frame. Low values of this rate were also observed on the torso and thighs, which leant on the flexible seat pad and which were pressed against it by the lap portion of the seat belt. The highest rates of growth of dynamic loads were recorded on the head, chiefly due to head impacts against parts of the vehicle interior.

6. Recapitulation

The values of the coefficient of growth of dynamic loads of dummy's parts were calculated and referred to the frame as the predominating component of the load-bearing structure of the vehicle under tests. The calculation results were approximated in most cases by function (6) and the curves thus obtained were plotted in a few graphs with a dashed line. The curves plotted in Fig. 5.1 show the general relationships between the growth of dynamic loads of the dummy and the load measured on the frame of the off-road passenger car during the car impact against the obstacle.

The curves plotted in Figs. 5.1 ÷ 5.3 and representing the functions that approximate the measurement results provide general information about the variations in the rate of growth of dynamic loads of the dummy in relation to the growth of dynamic loads of the frame with increasing vehicle impact speed. In particular:

- The rate of growth of dynamic loads of the head exceeded that recorded on the frame of the load-bearing system.
- The rate of growth of dynamic loads of the neck was lower than that recorded on the frame.
- The rates of growth of dynamic loads of the torso and thighs were significantly lower than that recorded on the frame.

The results obtained not only help in the work on improving the passive safety systems in vehicles with body-on-frame design but also indicate a possibility of defining the conditions of operation of such vehicles in terms of the probability of the bodily injuries that might occur in such conditions. A separate issue is the limited usability of results of such tests and analyses to the modelling and reconstruction of road accidents and to the prediction of effects of the accidents in respect of bodily injuries to vehicle occupants.

The research work carried out in this field is continued in order to acquire better and more comprehensive knowledge of variations in the processes of energy dissipation with increasing speeds of the vehicle impact against an obstacle.

References

[1] PROCHOWSKI L., ŻUCHOWSKI A.: *Właściwości nadwozia w zakresie pochłaniania energii podczas uderzenia samochodu w sztywną przeszkodę (Vehicle body properties in respect of energy absorption during a vehicle impact against a rigid obstacle)*. Zeszyty Naukowe Politechniki Świętokrzyskiej, Mechanika No. 84, Kielce 2006.

[2] DENIS V., CORNU P., HAMMOUNDA I., D'ACHON H., DISSOUBRAY X., SCHMITT V., RENOU CH., GUIGUEN N.: *French Study to Enhance Passive and Active Safety on Military Vehicles.* 20 Conference ESV, Lyon 2007.

[3] PN-ISO 6487: *Pojazdy drogowe. Techniki pomiarowe w testach zderzeniowych. Oprzyrządowanie (Road vehicles. Measurement techniques in crash tests. Instrumentation)*. 2005.

[4] HAGEL R., ZAKRZEWSKI J.: *Miernictwo dynamiczne (Dynamic metrology)*. WNT, Warszawa 1984.

[5] SWIESZNIKOW A. A.: *Podstawowe metody funkcji losowych (Basic methods of random functions)*. PWN, Warszawa 1965.

[6] WILENKIN S. J.: *Statystyczne metody badania układów sterowania automatycznego (Statistical methods of examining automatic control systems)*. WNT, Warszawa 1969.

[7] PROCHOWSKI L., ZIELONKA K., ŻUCHOWSKI A.: *Analiza ruchu ciała człowieka podczas zderzenia czołowego samochodu o ramowej konstrukcji nośnej z przeszkodą (The analysis of occupant motion in frontal barrier impact of a chassis frame vehicle)*. Journal of KONES 1/2011, Warszawa 2011.

[8] MATYJEWSKI M.: *Analiza i ocena technicznych sposobów zmniejszenia skutków wypadków drogowych (Analysis and evaluation of the technical methods to reduce the effects of road accidents)*. Prace Naukowe Politechniki Warszawskiej, No. 225, Mechanika, 2009.

The study was carried out within a research project of the Ministry of Science and Higher Education No. N509 403436.